THE JOURNAL OF PHYSICAL CHEMISTRY A

Article

pubs.acs.org/JPCA

Feasibility of Photosensitized Reactions with Secondary Organic Aerosol Particles in the Presence of Volatile Organic Compounds

Published as part of The Journal of Physical Chemistry virtual special issue "Veronica Vaida Festschrift".

Kurtis T. Malecha and Sergey A. Nizkorodov*

Department of Chemistry, University of California, Irvine, California 92697-2025, United States

Supporting Information

ABSTRACT: The ability of a complex mixture of organic compounds found in secondary organic aerosol (SOA) to act as a photosensitizer in the oxidation of volatile organic compounds (VOCs) was investigated. Different types of SOAs were produced in a smog chamber by oxidation of various biogenic and anthropogenic VOCs. The SOA particles were collected from the chamber onto an inert substrate, and the resulting material was exposed to 365 nm radiation in an air flow containing ~200 ppbv of limonene vapor. The mixing ratio of limonene and other VOCs in the flow was observed with a proton transfer reaction time-of-flight mass spectrometer (PTR-ToF-MS). The photosensitized uptake of limonene was observed for several SOA materials, with a lower limit for the reactive uptake coefficient on the scale of $\sim 10^{-5}$. The lower limit for the uptake coefficient under conditions of Los Angeles, California on the summer solstice at noon was estimated to be on the order of $\sim 10^{-6}$. Photoproduction of oxygenated VOCs (OVOCs) resulting from photodegradation of the SOA material also occurred in parallel with the photosensitized uptake of limonene. The estimated photosensitized limonene uptake rates by atmospheric SOA particles and vegetation surfaces appear to be too small to compete with the atmospheric oxidation of limonene by the hydroxyl radical or ozone. However, these processes could play a role in the leaf boundary layer where concentrations of oxidants are depleted and concentrations of VOCs are enhanced relative to the free atmosphere.

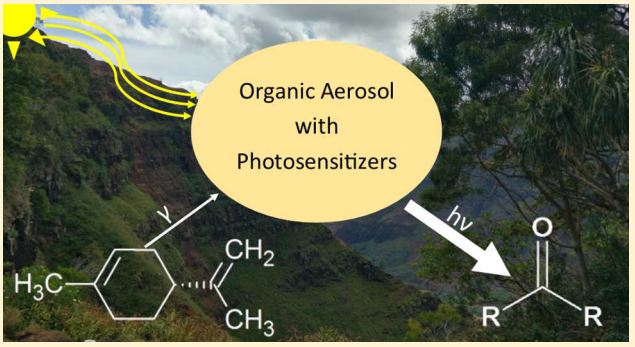

INTRODUCTION

Atmospheric secondary organic aerosol (SOA) is produced when atmospheric oxidants react with biogenic or anthropogenic volatile organic compounds (VOCs).[1] These reactions lead to successively lower volatility organics, which eventually partition into particles.[1] Further aging of the SOA particles can involve a variety of chemical and physical changes. For example, UV-induced photodegradation can reduce the average size and volatility of SOA compounds and serve as a source of small oxygenated VOCs, such as formic acid.[2−7] Alternatively, certain photochemical processes occurring at surfaces of aerosol particles and other environmental interfaces can also increase the average size and complexity of particulate organics.[8]

Recent work suggested an additional pathway to SOA particle growth through a photosensitized process in which VOCs are reactively taken up into particles in the presence of solar radiation and suitable photosenitizers.[9−15] Monge et al.[10] observed a size and mass increase of aerosol particles loaded with photosensitizers in the presence of limonene or isoprene and near-UV radiation. Aregahegn et al.[11] observed diameter growth of ammonium sulfate/glyoxal particles in the presence of various VOCs, and they attributed this growth to photosensitization processes involving imidazole-2-carboxaldehyde (IC).[16] In a follow-up study by Rossignol et al.,[13] the authors proposed a mechanism for the photosensitized oxidation of limonene on IC-containing particles, and they detected highly oxidized products of limonene with high-resolution mass spectrometry. Photosensitized oxidation of isoprene by IC was also observed in aqueous solution.[14] All of the previous studies involved various atmospheric aerosol proxies, such as IC-containing mixtures, and to the best of our knowledge, there is no published work on photosensitization by SOA.

The main goal of the experiments reported in this work is to verify whether similar photosensitized processes can occur in more atmospherically relevant systems, such as SOA produced by photooxidation of common biogenic and anthropogenic VOCs. With this project, the following questions are posed: (1) Does laboratory-generated SOA material have photosensitization properties? (2) What types of SOA materials show these properties? (3) Can the photosensitized uptake of VOCs into SOA particles and onto environmental surfaces under typical

Received: April 29, 2017
Revised: June 7, 2017
Published: June 9, 2017

DOI: 10.1021/acs.jpca.7b04066
J. Phys. Chem. A 2017, 121, 4961−4967

atmospheric conditions compete with oxidation of VOCs by gas-phase processes? To answer these questions, laboratory-generated SOA was collected on an inert substrate, and then it was irradiated in the presence of limonene vapor. We find that photosensitized uptake of limonene is possible on a broad range of SOA types; however, the estimated rate of photosensitized uptake under typical atmospheric conditions is considerably lower than the rates of gas-phase oxidation of limonene by OH and/or ozone. Photosensitized SOA + VOC processes on the vegetation could still play a role, especially in the immediate vicinity of leaves.

EXPERIMENTAL SECTION

Figure 1 shows an overview of the experimental approach. The SOA was generated in a ∼ 5 m^3 Teflon chamber in the absence of seed particles. The SOA formation was monitored with a scanning mobility particle sizer (SMPS; TSI model 3936), an NO_y monitor (Thermo Scientific model 42i-Y), an ozone monitor (Thermo Scientific model 49i), and, for select experiments, a proton transfer reaction time-of-flight mass spectrometer (PTR-ToF-MS; Ionicon model 8000).

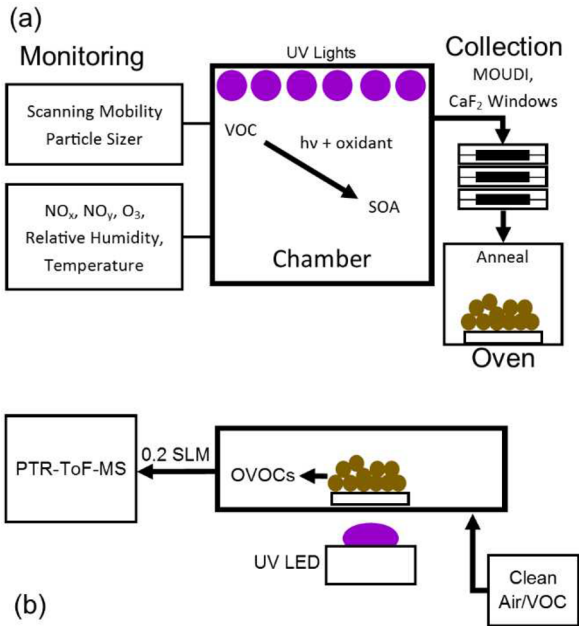

Figure 1. Overview of the SOA photosensitization experiments. (a) The SOA is prepared in the chamber, collected on an inert substrate, and annealed to remove volatile SOA components. (b) The sample is irradiated with a UV-light-emitting diode (LED) directly on the substrate in a photolysis flow cell. A collapsible Teflon bag provides either purge air or air containing a known mixing ratio of limonene. The limonene and photoproduced oxygenated VOCs (OVOCs) are monitored with the PTR-ToF-MS with an inlet flow of 0.2 standard liters per minute (SLM).

Table 1 lists the experimental conditions for the SOA generation. Relatively high mixing ratios of VOCs and oxidants were used in order to collect sufficient amounts of material for analysis. Hydrogen peroxide (H_2O_2) served as the OH precursor in low and high NO_x photooxidation experiments. H_2O_2 was added to the chamber by evaporating a measured volume of 30 wt % H_2O_2 aqueous solution in a cleaned glass trap with a stream of purge air. For high NO_x experiments, NO was added from a premixed gas cylinder to achieve a mixing ratio of ∼900 ppbv (parts per billion by volume). The VOC was added by evaporating a measured volume of pure VOC liquid or, in the case of naphthalene, a solution of 0.5 g mL^{-1} naphthalene in dichloromethane. The reagents' purity levels are listed in Table S1 in the Supporting Information (SI). The injected gases were mixed with a fan for several minutes to promote mixing, and the fan was turned off before turning on the UV lamps to minimize wall loss of particles. Forty-two UV−B lamps (centered at 310 nm; Solar Tec Systems model FS40T12/UVB) surrounding the chamber were turned on, and the aerosol formed for 1.5−4 h until the particle mass concentration reached a maximum as detected by the SMPS.

The SOA particles were collected with a micro orifice uniform deposit impactor (MOUDI; MSP Corporation model 110-R), which was modified to accommodate uncoated CaF_2 windows (Edmund Optics 25 mm diameter, 3 mm thickness) as substrates. Hundreds of micrograms of SOA material per window was collected, with stage 7 (0.32−0.56 μm particle size range) typically collecting the most mass. Stages 6 (0.56−1.0 μm) and 8 (0.18−0.32 μm) also usually collected sufficient amounts of material for experiments. The experimental results were found to be independent of the MOUDI collection stage, making it possible to use any of the MOUDI stages with sufficient mass of SOA on them. The windows were annealed overnight in a laboratory oven at 40 °C with ∼10 L/min of purge air flowing over the windows to drive off the more volatile species. Typical mass losses were a couple of percent of the total collected mass on a window, as confirmed by a Sartorius ME5-F microbalance (1 μg precision). If the annealing process was not performed, the OVOCs evaporating from the sample would provide too much background for the

Table 1. Summary of the SOA Samples Prepared for This Work[a]

precursor	oxidant(s)	no. of repeat chamber runs	precursor (ppmv)	H_2O_2 (ppmv)	NO (ppmv)	reaction time (h)	collection time (h)
NAP	OH, low NO_x	3	0.9	4	0	3.5	4
NAP	OH, high NO_x	3	0.9	4	0.9	3	4
LIM	OH, low NO_x	2	1	5	0	3.5	4.5
LIM	OH, high NO_x	2	1	5	0.9	1.5	3.5
ISO	OH, low NO_x	2	3	18	0	4	3.5
ISO	OH, high NO_x	2	3	18	0.9	3	3.5
GUA	OH, low NO_x	2	0.5	2	0	4	3
GUA	OH, high NO_x	2	0.5	2	0.9	3.5	3

[a]The precursors correspond to "NAP" = naphthalene, "LIM" = D-limonene ((4*R*)-1-methyl-4-(1-methylethenyl)-cyclohexene), "ISO" = isoprene (2-methylbuta-1,3-diene), and "GUA" = guaiacol (2-methoxyphenol). The oxidants correspond to "OH, low NO_x" = low NO_x conditions and "OH, high NO_x" = high NO_x conditions. Columns 4−6 correspond to approximate starting mixing ratios of precursors and oxidant(s).

DOI: 10.1021/acs.jpca.7b04066
J. Phys. Chem. A 2017, 121, 4961−4967

photosensitization experiments with the PTR-ToF-MS, which are described next.

A reference system containing a mixture of benzophenone (BP, a well-known photosensitizer)[17] and succinic acid (SA, with no known photosensitization properties) was prepared by casting a solution containing known amounts of these compounds in a 1:1 (v/v) methanol/acetone mixture onto a CaF_2 window, drying it and annealing it in the same way as was done for the SOA samples.

An annealed SOA or reference BP/SA sample window was placed into a custom-built glass flow cell with a connection to a ∼100 L Teflon bag that was filled with either purge air or a specified mixing ratio of limonene (typically ∼200 ppbv) for control and photosensitization experiments, respectively. The flow cell (Figure S2) represented a 15 mm i.d. tube, with a 30 mm long, 15 mm i.d. side arm, which was terminated with a #15 O-ring joint for connecting a CaF_2 window loaded with SOA or BP/SA. A sampling flow from the PTR-ToF-MS instrument was used to withdraw air from the bag and over the sample at 0.2 SLM.

A UV-LED and LED driver (Thorlabs, Inc. models M365LP1 and LEDD1B, respectively) with a wavelength centered at ∼365 nm, a full width at half-maximum of ∼10 nm, and a maximum power of ∼480 mW at 1.2 A current (measured with a Coherent Powermax PS19Q power sensor) was used to irradiate the material on the CaF_2 window. The spectral flux density experienced by the SOA sample was also verified using actinometry as described by Bunce et al.[18] The actinometry and direct power measurements agreed with each other to within a factor of 3 (power sensor/actinometry). This level of agreement is sufficient for the qualitative conclusions reached in this paper.

The limonene signal and the OVOCs resulting from the SOA material photodegradation were detected with the PTR-ToF-MS (drift tube voltage of 600 V, field strength of ∼135 Td, drift temperature of 60 °C, inlet flow of 0.2 SLM, and resolving power of $m/\Delta m \approx 5 \times 10^3$). The OVOC and limonene mixing ratios flowing over the sample and resulting from the irradiation were estimated using the built-in calculations of the PTR-ToF-MS viewer software from Ionicon Analytik (v.3.2.4.0), transmission curves created from a calibrated "TO-14" aromatics mix (Linde), and rate constants between the hydronium ion and the OVOCs/limonene from Zhao and Zhang.[19] These resulting estimations were calibrated with the PTR-ToF-MS for selected OVOCs. Details are given in the SI.

RESULTS AND DISCUSSION

Loss of Limonene and Formation of OVOCs. Figure 2 shows the result of a typical irradiation experiment in which selected OVOCs and limonene are observed in the PTR-ToF-MS before, during, and after irradiation with the presence of background limonene in the system. For each of these experiments, the window was inserted just before the 0 min mark, and a baseline count of the OVOCs (and the limonene) was recorded before the UV-LED was turned on. The UV-LED was turned off after observing a steady signal for the OVOCs (and limonene). The signal reached the baseline before inserting a new window. The limonene mixing ratio reproducibly decreased when the UV-LED was on and returned to the previous level after the UV-LED was turned off. During the irradiation period, several OVOCs' mixing ratios increased when the UV-LED was on.

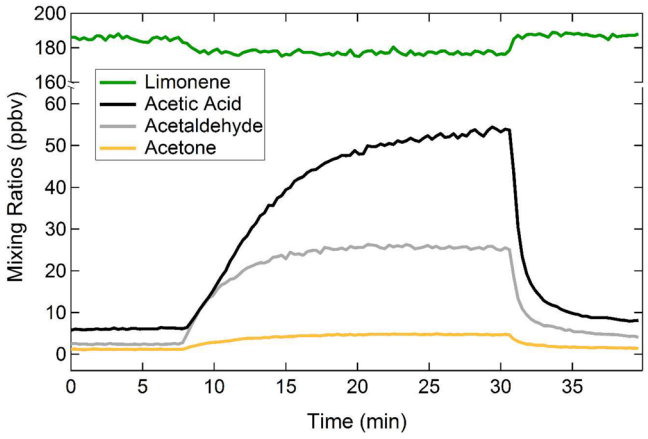

Figure 2. Example of photoinduced uptake of limonene and photoproduction of various OVOCs from the NAP/NO_x SOA observed with the PTR-ToF-MS. The UV-LED was turned on at ∼8 min and turned off at ∼30 min.

Most of the increase in OVOCs can be attributed to photodegradation of the SOA material.[7] In our previous experiments, which had a similar design but did not have limonene flowing over the SOA, the SOA photodegradation from 305 nm radiation was readily observed. In control experiments with the 365 nm light source, in the absence of limonene, the same nominal masses increased in abundance during irradiation in the PTR-ToF-MS traces as previously observed.[7] However, due to the much larger intensity of the 365 nm LED, the increase in the OVOC signals was considerably higher. Formic acid was observed as the major SOA photodegradation product, similar to the findings of our previous work.[7,20−22] In this work, the increase in formic acid from SOA photodegradation was so large that it often saturated the PTR-ToF-MS detector. Therefore, the formic acid signal is not shown in Figure 2.

In addition to the photodegradation of SOA resulting in OVOCs, there was evidence for photosensitized uptake of limonene on SOA. Specifically, it was observed that for selected SOA systems, there was a decrease in the counts of limonene to a steady state when the UV-LED was turned on. The decrease in signal was only a few percent, as shown in Figure 2. Table 2 lists the SOA systems probed in this work and the effective uptake coefficients (γ_{eff}) for limonene, which are defined as the fraction of limonene collisions with the surface that lead to a photosensitized reaction. Note that the uptake coefficients in Table 2 correspond to UV-LED power of 480 mW, and they scale linearly with the power. The formulas for converting the observed reduction in the limonene mixing ratios into effective uptake coefficients are provided in the SI.

As described in the SI, diffusion limitations on the observed uptake rate could be possible with the flow cell geometry and experimental conditions used in this work. To minimize possible diffusion limitations, the flow pattern was intentionally changed in selected experiments so that the flow was supplied directly onto the window with a bent 3 mm i.d. tube inserted inside of the flow cell. This modification did not change the observed uptake coefficient, suggesting that there was sufficient turbulent mixing in the flow cell, making diffusion limitations less important. The fact that the γ_{eff} values are reproducibly different for a variety of SOA types also suggests that the diffusion limitations are minimal. Nevertheless, the γ_{eff} values

DOI: 10.1021/acs.jpca.7b04066
J. Phys. Chem. A 2017, 121, 4961−4967

Table 2. Summary of the Results of the Photosensitization Experiments[a]

SOA system	effective uptake coefficient (γ_{eff})
BP/SA reference system	5.7×10^{-5}
NAP/OH, low NO_x	1.3×10^{-5}
NAP/OH, high NO_x	3.1×10^{-5}
LIM/OH, low NO_x	
LIM/OH, high NO_x	2.0×10^{-5}
ISO/OH, low NO_x	
ISO/OH, high NO_x	2.4×10^{-5}
GUA/OH, low NO_x	7.4×10^{-6}
GUA/OH, high NO_x	1.1×10^{-5}

[a]The effective uptake coefficient, γ_{eff}, is listed for each system that exhibited measurable photosensitization. Because of the possible diffusion limitations in the experiments, the values of γ_{eff} may represent the lower limits for the actual uptake coefficients. The γ_{eff} are calculated for an LED power of 480 mW; when scaled to more typical atmospheric conditions, γ_{eff} would be a factor of ~17 smaller. If γ_{eff} is not listed, the decrease in limonene was not detectable. BP/SA stands for the benzophenone/succinic acid mixture, the reference system, which is expected to have photosensitization properties.

listed in Table 2 should be regarded as lower limits for the actual uptake coefficient.

It is important to note that the loss of gas-phase carbon in limonene in Figure 2 is not balanced by the gain of gas-phase carbon in OVOC production; therefore, there is both photodegradation of SOA and a photosensitized uptake of limonene occurring simultaneously. For all SOA systems, the amount of carbon in the OVOCs produced was more than an order of magnitude larger than that in the reacted limonene. It is certainly possible that the photosensitized uptake produces similar OVOCs compared to the ones produced by SOA photodegradation, but photodegradation of SOA is a far more important source of OVOCs than the photosensitized reactions. We attempted to determine the mass lost (or gained) by the SOA sample by recording its change in mass; however, the change in mass was small and not reproducible.

All of the high NO_x SOA samples and all naphthalene and guaiacol SOA samples exhibited photosensitization capabilities in these experiments. These capabilities are likely from nitrogen-containing photosensitizers and aromatics, and these are produced during high NO_x SOA formation (except for the reference BP/SA system, which already has a known photosensitizer). Previous studies have shown that lab-generated SOA under high NO_x conditions and urban particulate matter contain nitrogen-containing species, carbonyls, and nitroaromatics.[23,24] The guaiacol high NO_x samples likely formed substituted nitroaromatic species during the SOA generation,[25] and nitroaromatics are capable of photosensitization.[26,27] On the other hand, the naphthalene and guaiacol low NO_x samples may have formed ring-substituted products during SOA formation,[28,29] which are likely photosensitizers.[26,27]

The reference BP/SA system with the known BP photosensitizer is important as it strongly suggests that the loss of limonene is driven by photosensitization. An alternative explanation for the loss of limonene would be secondary gas-phase photochemical processes involving free radicals. For example, acetaldehyde, acetone, and other OVOCs produced by SOA photodegradation could potentially photolyze in the gas phase, creating free radicals that then attack limonene. Based on our estimates, the 365 nm absorption cross sections and photolysis quantum yields for acetaldehyde, acetone, and other observed OVOCs are far too small to account for the observed loss rate of limonene. However, we cannot rule out the possibility that free radicals are produced on the surface and then escape in the gas phase, as observed in recent experiments with the IC photosensitizer by González Palacios et al.[15]

In the photosensitized reaction of particles containing IC and gaseous limonene, Rossignol et al.[13] were able to detect a number of oxidation products of limonene in the particles by high-resolution electrospray ionization mass spectrometry. Some of the same compounds were also detected in the gas phase in this study. For example, protonated masses corresponding to $C_8H_{12}O_3$, $C_{10}H_{16}O_2$, $C_9H_{14}O_3$, $C_{10}H_{14}O_3$, and $C_9H_{12}O_4$ were detected across multiple SOA systems, with $C_{10}H_{14}O_3$ often being the compound that increased the most during irradiation. The results suggest that photosensitized reactions of limonene on SOA particles likely occur by a similar mechanism to the reaction of limonene in IC.

Absorption Spectra of Limonene Reaction Products. VOCs that react in photosensitized reactions could potentially result in products that are light-absorbing and therefore contribute to the burden of brown carbon.[30,31] When the reference BP/SA system was exposed to both limonene and 365 nm radiation, a visual browning of the sample occurred reproducibly. The resulting brown film was dissolved in methanol and examined with UV–visible spectrophotometry (Figure 3). Another window containing BP/SA was exposed to

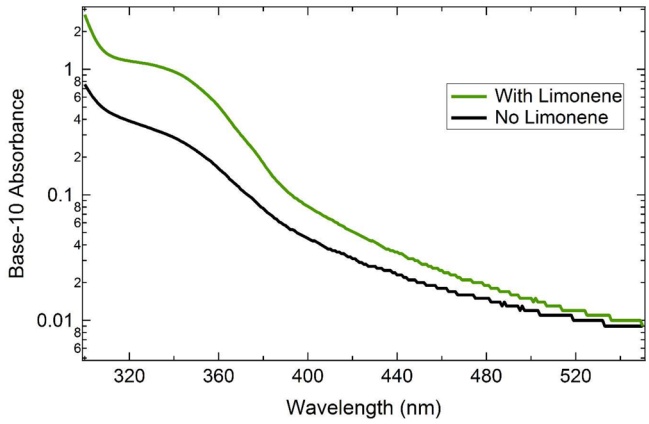

Figure 3. Comparison of the absorption spectra of the BP/SA reference system after irradiation for samples irradiated in the presence of limonene and without the presence of limonene.

just 365 nm radiation without limonene vapor, and no visual browning occurred. Each separate window for this control had the same amount of material deposited onto it, and each window's material was dissolved in the same amount of methanol. Even though no drastic changes in the shape of the absorption spectrum were observed (Figure 3), the increase in the strength of the absorbance and the visual browning of the sample was reproducible. The change in the absorbance and browning of the sample suggests that some of the products of the photosensitized reaction of limonene with BP/SA remained on the surface, in agreement with observations of Rossignol et al.[13] for the limonene + IC photosensitized reactions. Because the amount of the deposited limonene reaction products is unknown, it is not possible to estimate the mass absorption coefficient from these data. However, such a small absorbance change in the visible range suggests that the mass absorption coefficient is too small for the limonene photosensitized

DOI: 10.1021/acs.jpca.7b04066
J. Phys. Chem. A 2017, 121, 4961–4967

reaction products to act as efficient absorbers of visible solar radiation. The SOA samples exposed to UV radiation and limonene vapor showed no discernible change in optical properties (data not shown). This does not rule out the possibility that limonene photosensitized reaction products remain on the surface of SOA; all that it shows is that these products are not strongly light-absorbing.

Control Experiments. Several control experiments were performed in this study. A cleaned CaF_2 window was placed into the system and was irradiated while purge air was flowing through the system. There was no reduction in the limonene signal and only a minimal (<4% relative to the baseline) increase in each OVOC's signal. The same experiment was performed with a film of paraffin wax (which is not expected to contain any photosensitizers) on a cleaned CaF_2 window, and a similar result to the cleaned CaF_2 was observed.

The power output of the UV-LED was varied, and it was noted that the reduction in limonene signal during irradiation of the high NO_x SOA samples was linearly related to the power output of the UV-LED (Figure 4). This suggests that nonlinear

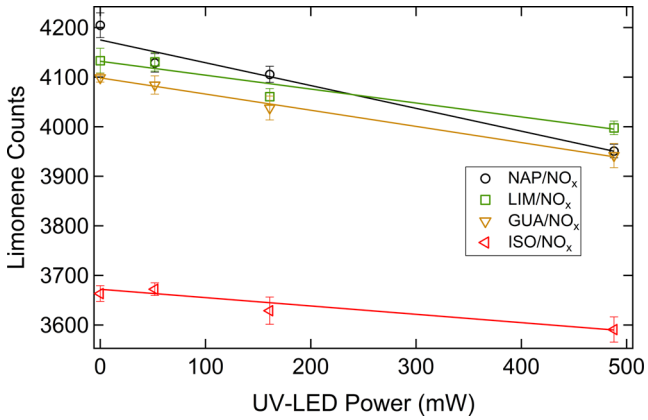

Figure 4. Regression plot of the limonene PTR-ToF-MS signal versus the UV-LED power for the high NO_x SOA systems. Error bars correspond to the 95% confidence level for the ion counts of protonated limonene. The reduction in the ion counts is linear with respect to the power of the UV-LED.

processes, such as two-photon absorption by the SOA material, are not likely to be responsible for the observations. This observation makes it possible to rescale the measured uptake coefficients listed in Table 2 to ambient conditions.

Finally, the background mixing ratio of the limonene flowing over the system was varied over 3 orders of magnitude from ~1 to ~500 ppbv of limonene. The uptake coefficient was independent of the limonene mixing ratio, consistent with a first-order process with respect to limonene.

Atmospheric Implications. The experiments described above were carried out at a relatively high power density of the 365 nm radiation (up to 480 mW/cm^2). The effective uptake coefficients listed in Table 2 correspond to the highest power density used in the experiments. Because the uptake of limonene by the irradiated SOA has a linear power dependence (Figure 4), we can estimate the uptake coefficient under more typical conditions by scaling the lamp's flux at 365 nm to that of the sun in the near-UV range (300−400 nm). In this estimation, we are assuming that visible and near-IR radiation (λ > 400 nm) do not contribute to the photosensitized chemistry because the SOA materials do not absorb strongly at these wavelengths.

This estimation was done for $\gamma_{eff} = 3 \times 10^{-5}$, which may represent the best-case scenario for photosensitized removal of limonene on SOA particles based on the data listed in Table 2. The sun's flux was calculated using the Quick TUV Calculator[32] with parameters corresponding to Los Angeles, California on the summer solstice at noon. A comparison of the sun and lamp's spectral flux densities and the parameters used for the TUV output can be found in the SI. The resulting scaling factor (lamp/sun = 17) translates to an effective $\gamma_{ambient}$ of 2×10^{-6} under these atmospheric conditions.

Would the estimated value of $\gamma_{ambient} = 2 \times 10^{-6}$ make the photosensitized loss of limonene on aerosol particles and ground surfaces competitive with gas-phase oxidation processes? To answer this question, the lifetime of limonene with respect to different loss processes was estimated (Table 3). The

Table 3. Lifetimes of Limonene with Respect to Different Atmospheric Sinks[a]

scenario	estimated lifetime
τ_{SOA}	>1 yr
τ_{OH}	100 min
τ_{Ozone}	170 min
$\tau_{Surface}$	26 h

[a]The subscripts correspond to "SOA" = deposition onto 300 nm monodisperse SOA particles at [SOA] = 15 μg m^{-3}, "OH" = gas-phase reaction of the hydroxyl radical at [OH] = 10^6 molecules cm^{-3}, "Ozone" = gas-phase reaction with ozone at [O_3] = 4.8×10^{11} molecules cm^{-3}, and "Surface" = deposition onto a vegetation surface.

details of the calculations are described in the SI. The lifetime for the loss of limonene in photosensitized reactions was estimated by modeling SOA particles as monodisperse with a particle diameter of 300 nm, particle material density of 1.4 g cm^{-3}, and particle mass concentration in air of 15 μg m^{-3}. The lifetimes for the loss of limonene in reactions with OH and O_3 assumed typical daytime atmospheric mixing ratios of these oxidants. The lifetime with respect to uptake onto vegetation surfaces coated with SOA material assumed 50 m^2 of available surface area over each square meter of the ground surface[33] and a boundary layer height (where species mix freely) of 500 m.

The predicted lifetimes of limonene with respect to the reactions with the hydroxyl radical and ozone are 100 and 170 min, respectively. The lifetime with respect to the photosensitized loss to SOA particles is orders of magnitude longer. As such, the photosensitized reaction of limonene with SOA particles cannot kinetically compete with the gas-phase oxidation processes. In terms of the rate with which mass is added to the particle, the SOA + VOC photosensitization process similarly cannot compete with the gas-phase oxidation followed by deposition, at least for VOCs that have high SOA yield. Because gas-phase oxidation of limonene produces SOA particles in high yields,[34] the rate of particle growth will be determined by the rate of limonene oxidation, which is faster in the gas phase. The situation may be different for VOCs that have low SOA yield, such as isoprene. However, for VOCs with high SOA yields, the photosensitized growth of particles proposed by Monge et al.[10] might be too slow compared to the growth from the normal gas-to-particle partitioning of limonene gas-phase oxidation products.

DOI: 10.1021/acs.jpca.7b04066
J. Phys. Chem. A 2017, 121, 4961−4967

Based on our estimations, the uptake of limonene onto vegetation surfaces ($\tau \approx 26$ h) may be more competitive with atmospheric gas-phase oxidation because of the higher available surface area provided by the vegetation surfaces. Because the uptake coefficients estimated in this study represent a lower limit for the actual uptake coefficients, the photosensitized uptake could be even faster. Such photosensitized reactions could be more relevant in the leaf boundary layer, where the concentrations of VOCs are higher and concentrations of oxidants are lower,[35] making the vegetation surface-driven photosensitized processes potentially important. This is a research avenue that should be explored as it may be another possible sink for freshly emitted VOCs in the atmosphere.

CONCLUSIONS

This exploratory study on the feasibility of photosensitized reactions involving SOA particles in the presence of gas-phase VOCs has shown that photoinduced uptake of VOCs is indeed experimentally observable on a variety of types of SOA particles. While previous observations of photosensitized loss of VOCs exist, they relied on simple model mixtures containing known photosensitizers. To the best of the authors' knowledge, this is the first time that photosensitized loss of VOCs on surfaces has been observed for more atmospherically relevant SOA. The experimentally determined lower limits for the effective uptake coefficients for the photosensitized loss of limonene on SOA particles are on the order of $\sim 10^{-5}$ under laboratory conditions or $\sim 10^{-6}$ under solar irradiation conditions corresponding to Los Angeles, California on the summer solstice at noon. The relatively small size of the uptake coefficient and insufficient surface area presented by ambient SOA particles make the resulting rate of the photosensitized loss of limonene on SOA particles considerably slower than the rate of the gas-phase oxidation of limonene by OH and O_3. However, the rate of photosensitized loss of limonene on vegetation surfaces coated with SOA material could be higher and potentially competitive with the gas-phase oxidation.

ASSOCIATED CONTENT

Supporting Information

The Supporting Information is available free of charge on the ACS Publications website at DOI: 10.1021/acs.jpca.7b04066.

Table of the reagents used for this work; the calibration procedures for the PTR-ToF-MS and the calibration factors for acetaldehyde, acetone, acetic acid, and limonene; the spectral flux densities of the UV-LED and the sun; and the derivation of the equations used in this work (PDF)

AUTHOR INFORMATION

Corresponding Author

*E-mail: nizkorod@uci.edu. Phone: +1-949-824-1262. Fax: +1-949-824-8671.

ORCID

Kurtis T. Malecha: 0000-0002-1438-7440

Sergey A. Nizkorodov: 0000-0003-0891-0052

Author Contributions

The experiments were planned jointly by K.T.M. and S.A.N. The experiments and analysis were performed by K.T.M. The manuscript was jointly written by both coauthors.

Notes

The authors declare no competing financial interest.

ACKNOWLEDGMENTS

K.T.M. thanks the National Science Foundation (NSF) for support from the Graduate Research Fellowship Program. The PTR-ToF-MS was acquired with NSF Grant MRI-0923323. The authors thank Dr. Manabu Shiraiwa for help with understanding diffusion limitations in reactive uptake experiments.

REFERENCES

(1) Pöschl, U. Atmospheric Aerosols: Composition, Transformation, Climate and Health Effects. *Angew. Chem., Int. Ed.* **2005**, *44*, 7520−7540.

(2) Henry, K. M.; Donahue, N. M. Photochemical Aging of α-Pinene Secondary Organic Aerosol: Effects of OH Radical Sources and Photolysis. *J. Phys. Chem. A* **2012**, *116*, 5932−5940.

(3) Epstein, S. A.; Blair, S. L.; Nizkorodov, S. A. Direct Photolysis of α-Pinene Ozonolysis Secondary Organic Aerosol: Effect on Particle Mass and Peroxide Content. *Environ. Sci. Technol.* **2014**, *48*, 11251−11258.

(4) Wong, J. P.; Zhou, S.; Abbatt, J. P. Changes in Secondary Organic Aerosol Composition and Mass Due to Photolysis: Relative Humidity Dependence. *J. Phys. Chem. A* **2015**, *119*, 4309−4316.

(5) Daumit, K. E.; Carrasquillo, A. J.; Sugrue, R. A.; Kroll, J. H. Effects of Condensed-Phase Oxidants on Secondary Organic Aerosol Formation. *J. Phys. Chem. A* **2016**, *120*, 1386−1394.

(6) Kroll, J. H.; Ng, N. L.; Murphy, S. M.; Flagan, R. C.; Seinfeld, J. H. Secondary Organic Aerosol Formation from Isoprene Photooxidation. *Environ. Sci. Technol.* **2006**, *40*, 1869−1877.

(7) Malecha, K. T.; Nizkorodov, S. A. Photodegradation of Secondary Organic Aerosol Particles as a Source of Small, Oxygenated Volatile Organic Compounds. *Environ. Sci. Technol.* **2016**, *50*, 9990−9997.

(8) Rapf, R. J.; Vaida, V. Sunlight as an Energetic Driver in the Synthesis of Molecules Necessary for Life. *Phys. Chem. Chem. Phys.* **2016**, *18*, 20067−20084.

(9) Handley, S. R.; Clifford, D.; Donaldson, D. J. Photochemical Loss of Nitric Acid on Organic Films: A Possible Recycling Mechanism for NO_x. *Environ. Sci. Technol.* **2007**, *41*, 3898−3903.

(10) Monge, M. E.; Rosenorn, T.; Favez, O.; Muller, M.; Adler, G.; Abo Riziq, A.; Rudich, Y.; Herrmann, H.; George, C.; D'Anna, B. Alternative Pathway for Atmospheric Particles Growth. *Proc. Natl. Acad. Sci. U. S. A.* **2012**, *109*, 6840−6844.

(11) Aregahegn, K. Z.; Noziere, B.; George, C. Organic Aerosol Formation Photo-Enhanced by the Formation of Secondary Photosensitizers in Aerosols. *Faraday Discuss.* **2013**, *165*, 123−134.

(12) De Laurentiis, E.; Socorro, J.; Vione, D.; Quivet, E.; Brigante, M.; Mailhot, G.; Wortham, H.; Gligorovski, S. Phototransformation of 4-Phenoxyphenol Sensitised by 4-Carboxybenzophenone: Evidence of New Photochemical Pathways in the Bulk Aqueous Phase and on the Surface of Aerosol Deliquescent Particles. *Atmos. Environ.* **2013**, *81*, 569−578.

(13) Rossignol, S.; Aregahegn, K. Z.; Tinel, L.; Fine, L.; Noziere, B.; George, C. Glyoxal Induced Atmospheric Photosensitized Chemistry Leading to Organic Aerosol Growth. *Environ. Sci. Technol.* **2014**, *48*, 3218−3227.

(14) Li, W. Y.; Li, X.; Jockusch, S.; Wang, H.; Xu, B.; Wu, Y.; Tsui, W. G.; Dai, H. L.; McNeill, V. F.; Rao, Y. Photoactivated Production of Secondary Organic Species from Isoprene in Aqueous Systems. *J. Phys. Chem. A* **2016**, *120*, 9042−9048.

(15) González Palacios, L.; Corral Arroyo, P.; Aregahegn, K. Z.; Steimer, S. S.; Bartels-Rausch, T.; Nozière, B.; George, C.; Ammann, M.; Volkamer, R. Heterogeneous Photochemistry of Imidazole-2-Carboxaldehyde: HO_2 Radical Formation and Aerosol Growth. *Atmos. Chem. Phys.* **2016**, *16*, 11823−11836.

(16) Tinel, L.; Dumas, S.; George, C. A Time-Resolved Study of the Multiphase Chemistry of Excited Carbonyls: Imidazole-2-Carboxaldehyde and Halides. *C. R. Chim.* **2014**, *17*, 801−807.
(17) Choudhry, G. G.; Roof, A. A. M.; Hutzinger, O. Mechanisms in Sensitized Photochemistry of Environmental Chemicals. *Toxicol. Environ. Chem. Rev.* **1979**, *2*, 259−302.
(18) Bunce, N. J.; Lamarre, J.; Vaish, S. P. Photorearrangement of Azoxybenzene to 2-Hydroxyazobenzene - a Convenient Chemical Actinometer. *Photochem. Photobiol.* **1984**, *39*, 531−533.
(19) Zhao, J.; Zhang, R. Y. Proton Transfer Reaction Rate Constants between Hydronium Ion (H_3O^+) and Volatile Organic Compounds. *Atmos. Environ.* **2004**, *38*, 2177−2185.
(20) Gomez, A. L.; Park, J.; Walser, M. L.; Lin, A.; Nizkorodov, S. A. UV photodissociation spectroscopy of oxidized undecylenic acid films. *J. Phys. Chem. A* **2006**, *110*, 3584.
(21) Walser, M. L.; Park, J.; Gomez, A. L.; Russell, A. R.; Nizkorodov, S. A. Photochemical Aging of Secondary Organic Aerosol Particles Generated from the Oxidation of D-Limonene. *J. Phys. Chem. A* **2007**, *111*, 1907−1913.
(22) Pan, X.; Underwood, J. S.; Xing, J. H.; Mang, S. A.; Nizkorodov, S. A. Photodegradation of Secondary Organic Aerosol Generated from Limonene Oxidation by Ozone Studied with Chemical Ionization Mass Spectrometry. *Atmos. Chem. Phys.* **2009**, *9*, 3851−3865.
(23) Nguyen, T. B.; Laskin, J.; Laskin, A.; Nizkorodov, S. A. Nitrogen-Containing Organic Compounds and Oligomers in Secondary Organic Aerosol Formed by Photooxidation of Isoprene. *Environ. Sci. Technol.* **2011**, *45*, 6908−6918.
(24) Kawamura, K.; Yasui, O. Diurnal Changes in the Distribution of Dicarboxylic Acids, Ketocarboxylic Acids and Dicarbonyls in the Urban Tokyo Atmosphere. *Atmos. Environ.* **2005**, *39*, 1945−1960.
(25) Chhabra, P. S.; Ng, N. L.; Canagaratna, M. R.; Corrigan, A. L.; Russell, L. M.; Worsnop, D. R.; Flagan, R. C.; Seinfeld, J. H. Elemental Composition and Oxidation of Chamber Organic Aerosol. *Atmos. Chem. Phys.* **2011**, *11*, 8827−8845.
(26) Turro, N. J.; Ramamurthy, V.; Scaiano, J. C. *Modern Molecular Photochemistry of Organic Molecules*; University Science Books: Sausalito, CA, 2010.
(27) Klán, P.; Wirz, J. Chemistry of Excited Molecules. *Photochemistry of Organic Compounds*; John Wiley & Sons, Ltd, 2009; pp 227−453.
(28) Lauraguais, A.; Coeur-Tourneur, C.; Cassez, A.; Deboudt, K.; Fourmentin, M.; Choel, M. Atmospheric Reactivity of Hydroxyl Radicals with Guaiacol (2-Methoxyphenol), a Biomass Burning Emitted Compound: Secondary Organic Aerosol Formation and Gas-Phase Oxidation Products. *Atmos. Environ.* **2014**, *86*, 155−163.
(29) Kautzman, K. E.; Surratt, J. D.; Chan, M. N.; Chan, A. W.; Hersey, S. P.; Chhabra, P. S.; Dalleska, N. F.; Wennberg, P. O.; Flagan, R. C.; Seinfeld, J. H. Chemical Composition of Gas- and Aerosol-Phase Products from the Photooxidation of Naphthalene. *J. Phys. Chem. A* **2010**, *114*, 913−934.
(30) Andreae, M. O.; Gelencser, A. Black Carbon or Brown Carbon? The Nature of Light-Absorbing Carbonaceous Aerosols. *Atmos. Chem. Phys.* **2006**, *6*, 3131−3148.
(31) Laskin, A.; Laskin, J.; Nizkorodov, S. A. Chemistry of Atmospheric Brown Carbon. *Chem. Rev.* **2015**, *115*, 4335−4382.
(32) Madronich, S. *Tropospheric Ultraviolet and Visible (TUV) Radiation Model*. https://www2.acom.ucar.edu/modeling/tropospheric-ultraviolet-and-visible-tuv-radiation-model (accessed April 14, 2017).
(33) Asner, G. P.; Scurlock, J. M. O.; Hicke, J. A. Global Synthesis of Leaf Area Index Observations: Implications for Ecological and Remote Sensing Studies. *Global Ecol. Biogeogr.* **2003**, *12*, 191−205.
(34) Griffin, R. J.; Cocker, D. R.; Flagan, R. C.; Seinfeld, J. H. Organic Aerosol Formation from the Oxidation of Biogenic Hydrocarbons. *J. Geophys. Res.: Atmos.* **1999**, *104*, 3555−3567.
(35) Holopainen, J. K. Multiple Functions of Inducible Plant Volatiles. *Trends Plant Sci.* **2004**, *9*, 529−533.

DOI: 10.1021/acs.jpca.7b04066
J. Phys. Chem. A 2017, 121, 4961−4967